

The non-monotonicity of moist adiabatic warming

Osamu Miyawaki^a

^a *Department of Geosciences, Union College, Schenectady New York, USA*

⁴ *Corresponding author:* Osamu Miyawaki, miyawako@union.edu

5 ABSTRACT: The moist adiabat is a useful first-order approximation of the tropical stratification
6 and thus governs fundamental properties of climate such as the static stability and the lapse
7 rate feedback. While total atmospheric latent heating increases monotonically with warming,
8 the resulting change in temperature along a moist adiabat is surprisingly non-monotonic with
9 surface temperature. This phenomenon has lacked a physical explanation. This paper presents a
10 thermodynamic explanation by decomposing the sensitivity of the moist adiabatic lapse rate into
11 two competing components: 1) A Cooling Term arising from the partial derivative of saturation
12 specific humidity with respect to temperature ($\partial q_s/\partial T$), which is proportional to q_s/T^2 via the
13 Clausius-Clapeyron relation, and 2) a Pressure Term arising from the partial derivative with respect
14 to pressure ($\partial q_s/\partial p$), which is proportional to q_s/p . The non-monotonicity arises because while
15 both terms grow with temperature due to the exponential increase of saturation specific humidity
16 (q_s), the $1/T^2$ prefactor on the Cooling Term suppresses its growth more strongly than the pressure-
17 related prefactor on the Pressure Term. This mechanism also explains the non-monotonic behavior
18 of convective buoyancy and vertical velocity.

1. Introduction

The Clausius-Clapeyron relation describes the potential for a warmer atmosphere to hold more water vapor (Emanuel 1994). This principle is the basis for the positive water vapor feedback, first quantified in early climate models (Manabe and Wetherald 1967), and for an increase in the latent heat released during convection as the climate warms. Consistent with these principles, the total latent heat released from convection increases monotonically with surface temperature (Fig. 1a).

In the tropics, convection couples the surface with the free troposphere. Although processes like convective entrainment influence the details of this coupling (Miyawaki et al. 2020), moist adiabatic adjustment serves as a useful first-order approximation (Held 1993). The top-heavy warming profile predicted by moist adiabatic adjustment (Fig. 1b) is a robust feature in climate models and observations, despite historical challenges in observational records (Vallis et al. 2015; Santer et al. 2005).

This warming profile is important because it increases atmospheric static stability, which influences convection (Neelin and Held 1987). This structure also defines the tropical lapse rate feedback, a key negative feedback for global climate sensitivity (Hansen et al. 1984). Given the monotonic increase in total latent heating (Fig. 1a), one might expect moist adiabatic warming to also be monotonic with surface temperature at all heights. However, it is a non-monotonic function of surface temperature at a fixed height (Fig. 1c). This non-monotonicity is independent of the vertical coordinate (Fig. A1). While Levine and Boos (2016) showed this non-monotonicity and its influence on zonal stationary circulations, a physical explanation for the non-monotonicity in moist adiabatic warming currently does not exist in the literature.

This raises the question: What physical mechanism drives this non-monotonic warming? This paper presents a thermodynamic explanation for the origins of non-monotonicity in moist adiabatic warming and its cascading effects on other convective properties. Section 2 develops the theory of non-monotonic warming. Section 3 explores the implications of this non-monotonicity for the dynamics of moist convection. Section 4 provides a summary and discussion.

2. Theory of Non-Monotonic Warming

The non-monotonic relationship between upper-tropospheric warming and surface temperature (Fig. 1) can be explained by analyzing the sensitivity of the moist adiabatic lapse rate, Γ_m , to




fig-1.png

FIG. 1. (a) The change in column-integrated saturation specific humidity resulting from a 4 K surface warming as a function of surface temperature (T_s). (b) Profiles of the moist adiabatic temperature response (ΔT) to a 4 K surface warming, plotted against pressure, for $T_s = 280, 290, 300, 310$, and 320 K. (c) The warming (ΔT) at 500, 400, 300, and 200 hPa as a function of T_s , showing a non-monotonic response where warming peaks at an intermediate temperature.

changes in surface temperature, T_s . To illustrate this, we start by defining the temperature profile, $T(z)$, in terms of its surface value, $T(0)$, and the lapse rate, $\Gamma(z) = -dT/dz$:

$$T(z) = T(0) - \int_0^z \Gamma(z') dz' \quad (1)$$

We apply Eq. (1) to a base state with surface temperature T_s and a perturbed state with surface temperature $T_s + \Delta T_s$. The warming at any height, $\Delta T(z)$, is the difference between these two profiles, $\Delta T(z) = T_{\text{pert}}(z) - T_{\text{base}}(z)$, which yields:

$$\Delta T(z) = \Delta T_s - \int_0^z \Delta \Gamma(z') dz' \quad (2)$$

where $\Delta \Gamma = \Gamma_{\text{pert}} - \Gamma_{\text{base}}$. For a small perturbation, the change in the lapse rate, $\Delta \Gamma$, can be approximated using a first-order Taylor expansion: $\Delta \Gamma \approx \frac{d\Gamma_m}{dT_s} \Delta T_s$. Substituting this into Eq. (2) gives:

$$\Delta T(z) \approx \Delta T_s - \left(\int_0^z \frac{d\Gamma_m}{dT_s} dz' \right) \Delta T_s \quad (3)$$

This establishes that the vertical structure of the warming anomaly (i.e., its deviation from the uniform surface warming) is controlled by the vertical integral of $d\Gamma_m/dT_s$, the sensitivity of the lapse rate to the surface temperature. Therefore, understanding the physical mechanisms that determine this sensitivity is the key to explaining the non-monotonicity of moist adiabatic warming.

We begin by deriving an expression for the moist adiabatic lapse rate from the first law of thermodynamics for a saturated, ascending air parcel, which is equivalent to the conservation of Moist Static Energy (MSE):

$$c_p dT + g dz + L_v dq_s = 0 \quad (4)$$

Here, c_p is the specific heat capacity of dry air, g is the acceleration due to gravity, z is height, L_v is the latent heat of vaporization, and q_s is the saturation specific humidity. To find the moist adiabatic lapse rate, $\Gamma_m = -dT/dz$, we divide Eq. (4) by dz :

$$c_p \frac{dT}{dz} + g + L_v \frac{dq_s}{dz} = 0 \quad (5)$$

Substituting $dT/dz = -\Gamma_m$ and solving for Γ_m yields:

$$\Gamma_m = \frac{g}{c_p} + \frac{L_v}{c_p} \frac{dq_s}{dz} = \Gamma_d + \frac{L_v}{c_p} \frac{dq_s}{dz} \quad (6)$$

where Γ_d is the dry adiabatic lapse rate. For simplicity, and following common theoretical practice, Γ_d , L_v , and c_p are assumed to be constant. Then the sensitivity of the lapse rate to surface

74 temperature is controlled entirely by the sensitivity of the vertical moisture gradient:

$$\frac{d\Gamma_m}{dT_s} = \frac{L_v}{c_p} \frac{d}{dT_s} \left(\frac{dq_s}{dz} \right) \quad (7)$$

75 We can decompose the moisture gradient, dq_s/dz , into two components using the chain rule, as q_s
76 is a function of temperature T and pressure p :

$$\frac{dq_s}{dz} = \frac{\partial q_s}{\partial T} \frac{dT}{dz} + \frac{\partial q_s}{\partial p} \frac{dp}{dz} \quad (8)$$

77 Substituting the definitions of the moist lapse rate ($dT/dz = -\Gamma_m$) and hydrostatic balance ($dp/dz =$
78 $-\rho g$, where ρ is the density of air) allows the moisture gradient to be expressed as the sum of a
79 Cooling Term and a Pressure Term:

$$\frac{dq_s}{dz} = \underbrace{-\Gamma_m \frac{\partial q_s}{\partial T}}_{\text{Cooling Term}} + \underbrace{\left(-\rho g \frac{\partial q_s}{\partial p} \right)}_{\text{Pressure Term}} \quad (9)$$

80 The Cooling Term represents the decrease in water vapor due to the parcel cooling as it rises
81 and expands. The Pressure Term represents the increase in water vapor due to the decrease in
82 ambient pressure as the parcel rises. Substituting this decomposition back into Eq. (7) allows us
83 to decompose the total sensitivity, $d\Gamma_m/dT_s$, into the sum of contributions from these two terms.
84 They have opposing effects on the total sensitivity (Fig. 2). The Cooling Term acts to decrease Γ_m
85 with warming (Fig. 2b), while the Pressure Term acts to increase Γ_m with warming (Fig. 2c).

86 The opposing effects of these two terms on the lapse rate translate into competing contributions
87 to the overall warming profile. Integrating the Cooling Term's sensitivity reveals a warming
88 contribution that amplifies monotonically with increasing T_s at all heights (Fig. 3a, 3b). In contrast,
89 integrating the Pressure Term's sensitivity reveals a contribution that acts to cool the atmosphere
90 relative to the surface, and this cooling effect becomes stronger as T_s increases (Fig. 3c, 3d).
91 Physically, this occurs because a decrease in ambient pressure favors the vapor phase over condensed
92 phases, which means the Pressure Term contributes to a decrease in latent heat release from
93 condensation compared to a hypothetical alternative where temperature were to decrease without
94 a corresponding decrease in pressure. The total warming anomaly, $\Delta T_{\text{anomaly}}(z) = \Delta T(z) - \Delta T_s$, is

95 the sum of these two opposing effects:

$$\Delta T_{\text{cool}}(z) \approx -\Delta T_s \int_0^z \frac{d}{dT_s} \left(\frac{L_v}{c_p} \left(-\Gamma_m \frac{\partial q_s}{\partial T} \right) \right) dz' \quad (10)$$

$$\Delta T_{\text{pres}}(z) \approx -\Delta T_s \int_0^z \frac{d}{dT_s} \left(\frac{L_v}{c_p} \left(-\rho g \frac{\partial q_s}{\partial p} \right) \right) dz' \quad (11)$$

$$\Delta T_{\text{anomaly}}(z) = \Delta T_{\text{cool}}(z) + \Delta T_{\text{pres}}(z) \quad (12)$$

96 The non-monotonic behavior of moist adiabatic warming is thus a consequence of the competition
97 between these two opposing effects.

98 The reason for the eventual dominance of the Pressure Term's temperature sensitivity lies in its
99 temperature scaling relative to the Cooling Term. We can approximate the partial derivatives of
100 specific humidity using the Clausius-Clapeyron relation and the ideal gas law:

$$\frac{\partial q_s}{\partial T} \approx q_s \frac{L_v}{R_v T^2} \quad (13)$$

$$\frac{\partial q_s}{\partial p} \approx -\frac{q_s}{p} \quad (14)$$

101 where R_v is the gas constant for water vapor. Substituting these approximations into Eq. (9) gives:

$$\frac{dq_s}{dz} \approx -\Gamma_m \left(q_s \frac{L_v}{R_v T^2} \right) - \rho g \left(-\frac{q_s}{p} \right) \approx -q_s \left(\Gamma_m \frac{L_v}{R_v T^2} \right) + q_s \left(\frac{\rho g}{p} \right) \quad (15)$$

102 Using the ideal gas law for moist air, $p \approx \rho R_d T_v$ (where T_v is the virtual temperature), the pressure-
103 related term in Eq. (15) can be rewritten:

$$\frac{dq_s}{dz} \approx -q_s \left(\frac{\Gamma_m L_v}{R_v T^2} \right) + q_s \left(\frac{g}{R_d T_v} \right) \quad (16)$$

104 Both terms scale with the saturation specific humidity, q_s , which increases exponentially with tem-
105 perature. However, they are also multiplied by prefactors with different temperature dependencies.

106 The Cooling Term is modulated by a prefactor that scales as $1/T^2$. This dampens the exponential
107 increase in the Cooling Term with surface warming. Γ_m in the numerator of the Cooling Term
108 prefactor further modulates the exponential increase because Γ_m decreases with warming. The
109 Pressure Term is modulated by a prefactor that scales as $1/T_v$. Thus the Pressure Term prefactor

110 is a weaker function of temperature than the Cooling Term prefactor (Fig. 4). Consequently, as T_s
 111 rises, the rapid decay of the Cooling Term's prefactor mutes the effect of increasing q_s relative to
 112 the Pressure Term. This allows the Pressure Term's influence on the lapse rate to eventually catch
 113 up to that of the Cooling Term. The differing sensitivities of these two terms to temperature cause
 114 the warming to first strengthen and then weaken with T_s .

131 3. Implications of non-monotonicity in moist adiabatic warming on convection

132 The non-monotonic warming of a moist adiabat has implications for the dynamics of convection.
 133 For example, Romps (2016) showed that parcel buoyancy at the tropopause is a non-monotonic
 134 function of surface temperature. Romps' explanation is that as surface temperature increases
 135 the parcel's enthalpy anomaly is increasingly partitioned into a latent enthalpy (moisture) anomaly
 136 rather than a sensible enthalpy (temperature) anomaly. Since buoyancy is driven by the temperature
 137 anomaly between the rising parcel and its environment, the shift from sensible to latent enthalpy
 138 anomaly with warming leads to the tropopause buoyancy and thus CAPE to peak at an intermediate
 139 temperature. Here, we provide an alternative perspective of the non-monotonicity in buoyancy
 140 based on the sensitivity of the vertical moisture gradient ($\frac{dq_s}{dz}$) to warming.

141 We model buoyancy (B) as the normalized virtual temperature difference between a non-
 142 entraining parcel ($T_{v,p}$) and the environment ($T_{v,e}$). For simplicity, we will use standard tem-
 143 perature:

$$B(z) \approx \frac{g}{T_e(z)} (T_p(z) - T_e(z)) \quad (17)$$

144 As before, we express temperature profiles in terms of T_s and the integral of their respective lapse
 145 rates. We assume the parcel follows a moist adiabatic lapse rate, Γ_m , while the environment follows
 146 an entraining lapse rate, Γ_e .

$$T_p(z) = T_s - \int_0^z \Gamma_m(z') dz' \quad (18)$$

$$T_e(z) = T_s - \int_0^z \Gamma_e(z') dz' \quad (19)$$

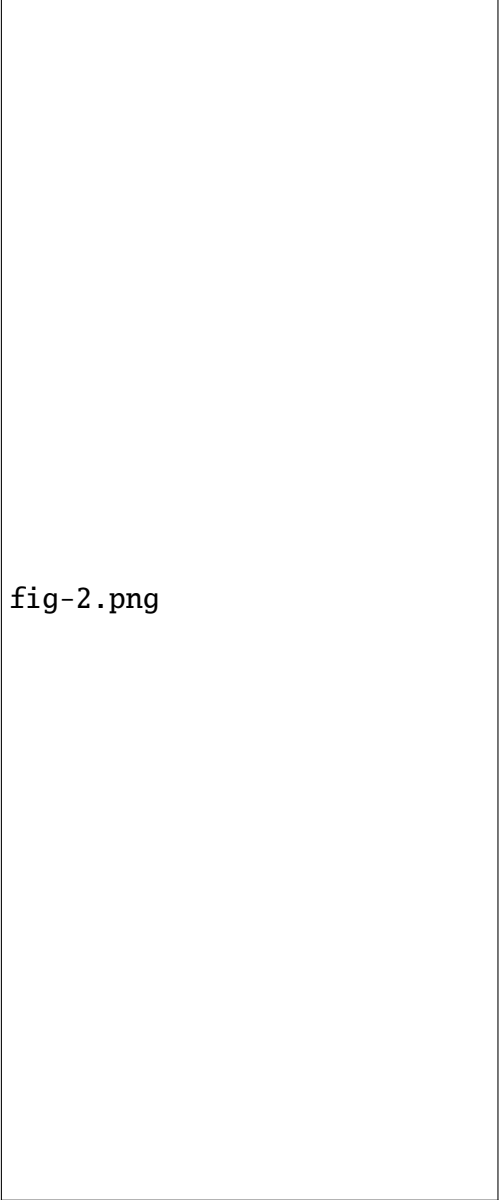


fig-2.png

115 FIG. 2. The sensitivity of the moist adiabatic lapse rate to a change in surface temperature, $\partial\Gamma_m/\partial T_s$, exhibits
116 a non-monotonic structure as a function of height and temperature (a). This structure arises from the competition
117 between two opposing physical effects. The Cooling Term (b), which represents the effect of condensation from
118 adiabatic cooling, is a negative contribution at all temperatures. The Pressure Term (c), which represents the
119 effect of decreasing pressure with height, is a positive contribution. The non-monotonicity of the total sensitivity
120 arises because the positive contribution from the Pressure Term grows more rapidly with T_s than the negative
121 contribution from the Cooling Term.

fig-3.png

FIG. 3. Warming is decomposed into contributions from the Cooling Term and the Pressure Term. (a) The vertical profile of the warming contribution from the Cooling Term for select T_s . (b) The warming contribution from the Cooling Term at fixed heights as a function of surface temperature. This term provides a warming effect that increases monotonically with temperature. (c) The vertical profile of the relative cooling contribution from the Pressure Term. (d) The relative cooling from the Pressure Term at fixed heights. Both the Cooling and Pressure terms become stronger as the surface temperature increases.

fig-4.png

FIG. 4. The (a) Cooling Prefactor, $\Gamma_m L_v / (R_v T^2)$, and (b) Pressure Prefactor, $g / (R_d T_v)$, as a function of height and surface temperature. The Cooling Prefactor weakens strongly with temperature due to its $1/T^2$ dependence. In contrast, the Pressure Prefactor weakens more slowly due to its $1/T_v$ dependence.

Substituting Eq. (18) and (19) into the definition of buoyancy (Eq. 17) yields:

$$B(z) \approx \frac{g}{T_e(z)} \int_0^z (\Gamma_e(z') - \Gamma_m(z')) dz' \quad (20)$$

The lapse rate of the entraining environment, Γ_e , can be derived from the conservation of entraining moist static energy following Eq. (B18) in Roms (2016). This yields:

$$\Gamma_e = \frac{g}{c_p} + \frac{L_v}{c_p(1+a)} \frac{dq_s}{dz} \quad (21)$$

where a is a dimensionless entrainment parameter. Here, we use $a = 0.2$ following Roms (2016). The difference between the environmental and parcel lapse rates is therefore directly proportional to the vertical moisture gradient:

$$\Gamma_e(z') - \Gamma_m(z') = \left(\frac{1}{1+a} - 1 \right) \frac{L_v}{c_p} \frac{dq_s}{dz} = -\frac{a}{1+a} \frac{L_v}{c_p} \frac{dq_s}{dz} \quad (22)$$

Substituting Eq. (22) into Eq. (20) shows that the same physical mechanism used to explain the non-monotonicity in moist adiabatic warming applies for buoyancy:

$$B(z) = -\frac{g}{T_e(z)} \left(\frac{a}{1+a} \frac{L_v}{c_p} \right) \int_0^z \frac{dq_s}{dz'} dz' \quad (23)$$

This shows that buoyancy is directly proportional to the vertical integral of the moisture gradient, dq_s/dz . Since dq_s/dz is composed of the competing Cooling and Pressure terms, it follows that buoyancy is governed by the same mechanism.

Numerical calculations confirm this expectation. The results show that buoyancy at a fixed height first increases and then decreases as the T_s increases (Fig. 5). Decomposing the total buoyancy into the two components reveals the source of this behavior (Fig. 6). The total buoyancy, B_{total} , is the sum of the contributions from the Cooling Term (B_{cool}) and the Pressure Term (B_{pres}):

$$B_{\text{cool}}(z) = -\frac{g}{T_e(z)} \left(\frac{a}{1+a} \frac{L_v}{c_p} \right) \int_0^z \left(-\Gamma_m \frac{\partial q_s}{\partial T} \right) dz' \quad (24)$$

$$B_{\text{pres}}(z) = -\frac{g}{T_e(z)} \left(\frac{a}{1+a} \frac{L_v}{c_p} \right) \int_0^z \left(-\rho g \frac{\partial q_s}{\partial p} \right) dz' \quad (25)$$

$$B_{\text{total}}(z) = B_{\text{cool}}(z) + B_{\text{pres}}(z) \quad (26)$$

The Cooling Term provides a positive buoyancy contribution that increases monotonically with surface temperature, while the Pressure Term provides a negative buoyancy contribution that also grows in magnitude. The sum of these two opposing effects produces the non-monotonic behavior of buoyancy.

This non-monotonic behavior of buoyancy extends to the strength of the convective updraft. We model the updraft's specific kinetic energy, $\frac{1}{2}w^2$, using Eq. (1) from Del Genio et al. (2007):

$$\frac{d}{dz} \left(\frac{1}{2} w^2 \right) = a' B(z) - (1 + b') \epsilon(z) w^2 \quad (27)$$

where a' and b' are dimensionless constants. We use $a' = 1/6$ and $b' = 2/3$ following Del Genio et al. (2007). $\epsilon(z)$ is the fractional entrainment rate, which is calculated following Eq. (3) in Romps (2016) with precipitation efficiency $PE = 0.35$. Since $w(z)$ is determined by the integral of the

171 net force, which includes buoyancy, we expect the non-monotonic dependence on T_s extends to the
 172 vertical velocity profile as well.

173 Numerically integrating Eq. (27) confirms this expectation (Fig. 7). The resulting vertical
 174 velocity profiles exhibit a clear non-monotonic dependence on T_s . Because Eq. (27) is non-linear,
 175 the contributions from the two buoyancy terms are not simply additive. We therefore isolate
 176 the influence of each term by first calculating the velocity driven by the Cooling Term's positive
 177 buoyancy alone (w_{cool}), and then calculating the effect of the Pressure Term (w_{pres}) as the residual
 178 required to recover the total velocity (w_{total}):

$$\frac{d}{dz} \left(\frac{1}{2} w_{\text{cool}}^2 \right) = a' B_{\text{cool}}(z) - (1 + b') \epsilon(z) w_{\text{cool}}^2 \quad (28)$$

$$w_{\text{pres}}(z) = w_{\text{total}}(z) - w_{\text{cool}}(z) \quad (29)$$

179 This decomposition (Fig. 8) shows that the monotonically increasing velocity from the Cooling
 180 Term is counteracted by an increasingly strong opposing effect from the Pressure Term, resulting
 181 in the non-monotonic total response.

fig-5.png

182 FIG. 5. (a) Vertical profiles of buoyancy for an undiluted parcel ascending through an environment set by an
 183 entraining plume, calculated for several surface temperatures. (b) Buoyancy at fixed heights as a function of
 184 surface temperature. The entraining environmental profile follows Roms (2016).

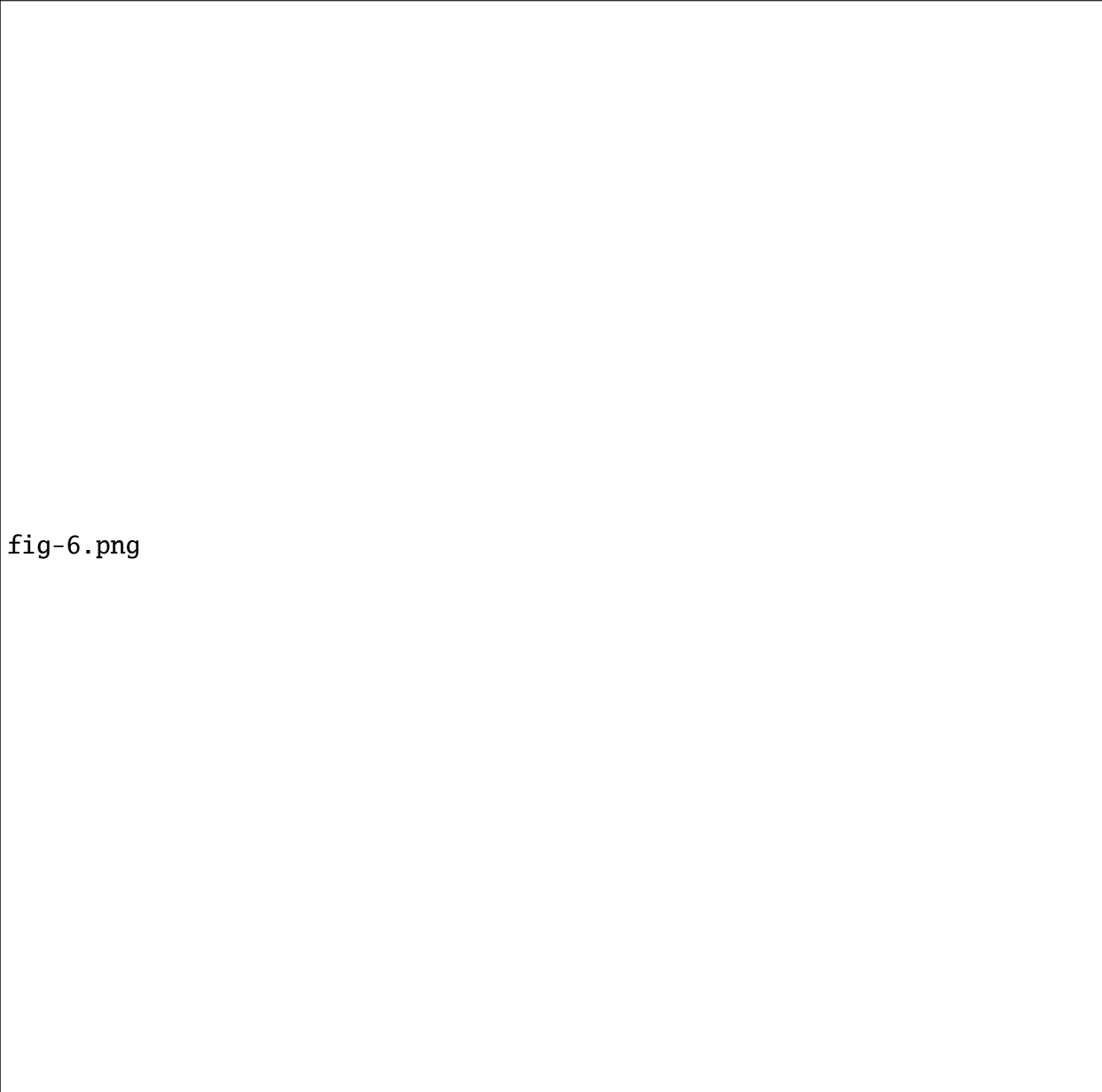


fig-6.png

185 FIG. 6. The total buoyancy from Fig. 5 is decomposed into contributions from the Cooling and Pressure terms.
186 (a,b) The contribution to buoyancy from the Cooling Term, which provides a positive, monotonically increasing
187 forcing. (c,d) The contribution from the Pressure Term, which provides a negative (suppressing) forcing that
188 grows in magnitude with temperature.

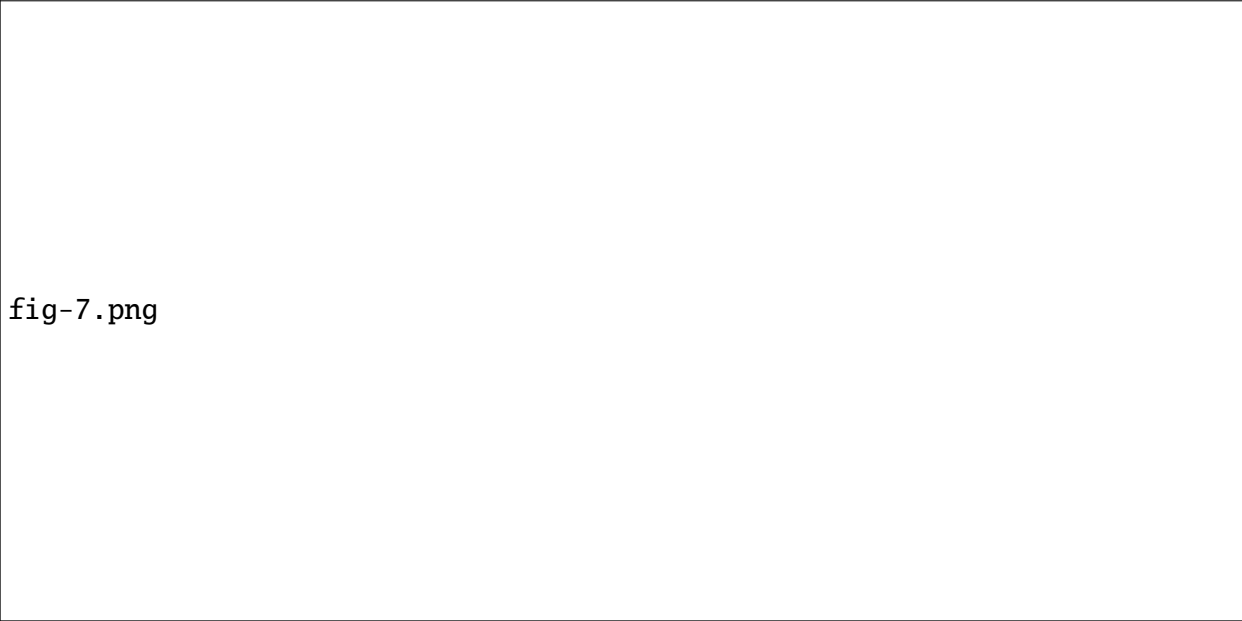


fig-7.png

189 FIG. 7. (a) Vertical profiles of updraft velocity, calculated by numerically integrating Eq. (27) using the total
190 buoyancy from Fig. 5. (b) Updraft velocity at fixed heights as a function of surface temperature. The velocity
191 exhibits a clear non-monotonic dependence on surface temperature, consistent with the behavior of buoyancy.

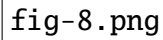


fig-8.png

FIG. 8. The total vertical velocity is decomposed to show the influence of the Cooling and Pressure terms. (a,b) The velocity profile resulting from the positive buoyancy of the Cooling Term alone. (c,d) The effect of the Pressure Term on velocity, calculated as the residual between the total velocity and the velocity from the Cooling Term.

4. Summary and Discussion

This paper presents a thermodynamic explanation for the non-monotonicity of moist adiabat warming. The non-monotonicity arises through the competing influences of a Cooling Term and a Pressure Term on the sensitivity of the moist adiabatic lapse rate. While both terms are proportional to the saturation specific humidity (q_s), which increases nearly exponentially with temperature, they are modulated by prefactors with different inverse temperature dependencies. The Cooling Term is proportional to q_s/T^2 , while the Pressure Term is proportional to q_s/T . The non-monotonic response arises because the stronger $1/T^2$ dependence of the Cooling Term's prefactor causes its influence to weaken relative to that of the Pressure Term as the climate warms, leading to a crossover in their relative sensitivity to surface warming. The same mechanism for lapse rate sensitivity cascades to explain the non-monotonic behavior of convective buoyancy and vertical velocity as a function of T_s .

Our findings on buoyancy complement the work of Romps (2016), who first explained the non-monotonicity of CAPE. The two studies offer different but complementary insights. Romps (2016) focused on explaining the non-monotonicity of buoyancy at the tropopause as a proxy for CAPE. Here, we focus on explaining the non-monotonicity of buoyancy at any fixed height. We also provide a different perspective on the source of non-monotonicity that arises from the competition in the sensitivity of a Cooling Term that favors condensation and a Pressure Term, driven by decreasing ambient pressure, that opposes it.

The non-monotonicity of moist adiabatic warming may have additional implications for climate, such as the organization of convection and the large-scale circulation response to warming. The non-monotonicity of moist adiabatic warming would drive a non-monotonic change in the meridional and zonal temperature gradients. This could serve as a thermodynamically driven hypothesis for understanding state dependence in the response of Hadley and Walker Cells to warming.

Acknowledgments. I thank Andrew Williams, Jiawei Bao, Jonah Bloch-Johnson, Martin Singh, and Stephen Po-Chedley for helpful discussions.

Data availability statement. All scripts used for analysis and plots in this paper are available at <https://github.com/omiyawaki/miyawaki-2025-nonmonotonic-moist-adiabat>. They will also be archived on Zenodo upon publication.

APPENDIX A

Calculation of Moist Adiabatic Profiles

The moist adiabatic profiles are calculated numerically by assuming that moist static energy (MSE) is conserved, where:

$$\text{MSE} = c_p T + g z + L_v q_s \quad (\text{A1})$$

Here, T is temperature, z is height, p is pressure, q_s is the saturation specific humidity, g is the acceleration due to gravity, c_p is the specific heat of dry air at constant pressure, and L_v is the latent heat of vaporization. All thermodynamic constants are defined in Table A1. Saturation vapor pressure is calculated using Eq. (10) in Bolton (1980).

The calculation proceeds in discrete vertical steps of Δz (100 m). For a given surface temperature (T_s) and surface pressure (p_s), MSE is calculated at the surface ($z = 0$) and is held constant over height. At each subsequent height step z_{i+1} , the pressure p_{i+1} is first calculated using hydrostatic balance. Then, a numerical root-finding algorithm (`scipy.optimize.root_scalar` with the Brentq method) is used to find the temperature T_{i+1} that satisfies the condition that the MSE at ($T_{i+1}, p_{i+1}, z_{i+1}$) is equal to the surface MSE.

To demonstrate that the non-monotonic warming is independent of the vertical coordinate, the results are also presented in pressure coordinates (Fig. A1). These profiles are obtained by interpolating the temperature profiles for the base and perturbed climates onto a common pressure grid. The warming profile in pressure coordinates, $\Delta T(p)$, is the difference between these two interpolated temperature profiles.

TABLE A1. Thermodynamic constants used in the calculation of moist adiabatic profiles.

Symbol	Description	Value	Units
g	Acceleration due to gravity	9.81	m s^{-2}
c_p	Specific heat of dry air	1005.7	$\text{J kg}^{-1} \text{K}^{-1}$
R_d	Gas constant for dry air	287.05	$\text{J kg}^{-1} \text{K}^{-1}$
R_v	Gas constant for water vapor	461.5	$\text{J kg}^{-1} \text{K}^{-1}$
ϵ	Ratio of gas constants (R_d/R_v)	0.622	dimensionless
p_s	Reference surface pressure	100,000	Pa
L_v	Latent heat of vaporization	2.501×10^6	J kg^{-1}

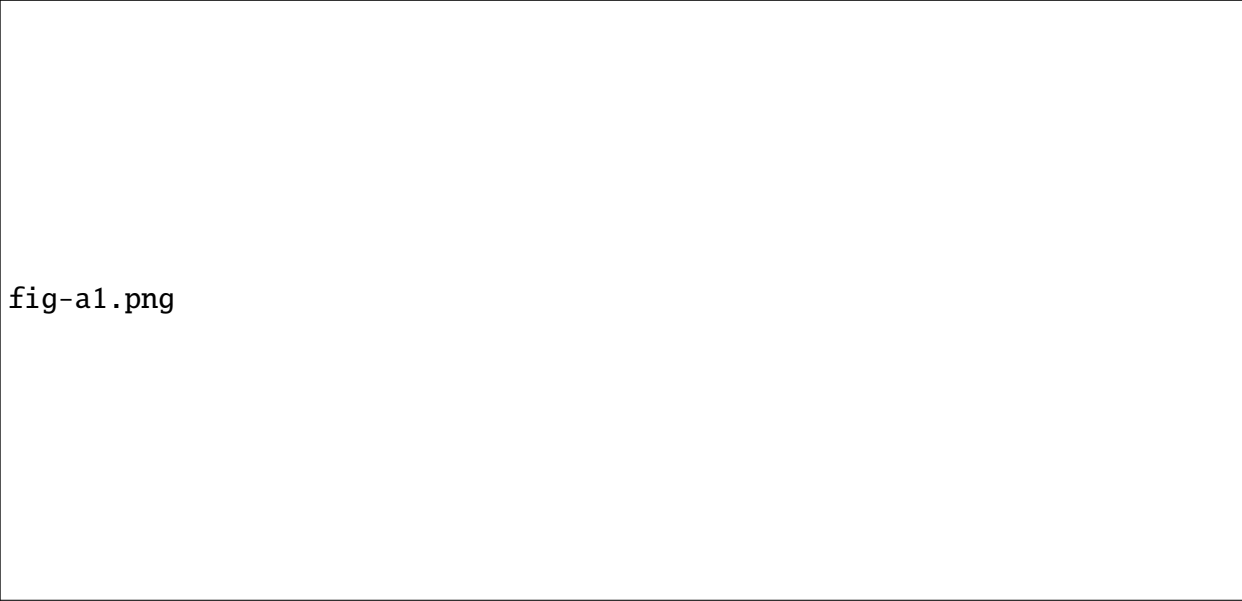


fig-a1.png

244 FIG. A1. The moist adiabatic warming response to a 4 K surface warming in pressure coordinates. (a) Vertical
245 profiles of the temperature response (ΔT) as a function of pressure for surface temperatures (T_s) of 280, 290,
246 300, 310, and 320 K. (b) The warming (ΔT) at fixed pressure levels of 500, 400, 300, and 200 hPa as a function
247 of T_s . The non-monotonic behavior seen in height coordinates (Fig. 1c) is also evident in pressure coordinates.

References

- Bolton, D., 1980: The computation of equivalent potential temperature. *Mon. Weather Rev.*, **108** (7), 1046–1053.
- Del Genio, A. D., M.-S. Yao, and J. Jonas, 2007: Will moist convection be stronger in a warmer climate?: CONVECTION STRENGTH IN a WARMER CLIMATE. *Geophys. Res. Lett.*, **34** (16).
- Emanuel, K. A., 1994: *Atmospheric Convection*. Oxford University Press.
- Hansen, J., A. Lacis, D. Rind, G. Russell, P. Stone, I. Fung, R. Ruedy, and J. Lerner, 1984: Climate sensitivity: Analysis of feedback mechanisms. *Climate Processes and Climate Sensitivity*, American Geophysical Union (AGU), 130–163.
- Held, I. M., 1993: Large-scale dynamics and global warming. *Bull. Am. Meteorol. Soc.*, **74** (2), 228–242.
- Levine, X. J., and W. R. Boos, 2016: A mechanism for the response of the zonally asymmetric subtropical hydrologic cycle to global warming. *J. Clim.*, **29** (21), 7851–7867.
- Manabe, S., and R. T. Wetherald, 1967: Thermal equilibrium of the atmosphere with a given distribution of relative humidity. *J. Atmos. Sci.*, **24** (3), 241–259.
- Miyawaki, O., Z. Tan, T. A. Shaw, and M. F. Jansen, 2020: Quantifying key mechanisms that contribute to the deviation of the tropical warming profile from a moist adiabat. *Geophys. Res. Lett.*, **47** (20), e2020GL089136.
- Neelin, J. D., and I. M. Held, 1987: Modeling tropical convergence based on the moist static energy budget. *Mon. Weather Rev.*, **115** (1), 3–12.
- Romps, D. M., 2016: Clausius–Clapeyron scaling of CAPE from analytical solutions to RCE. *J. Atmos. Sci.*, **73** (9), 3719–3737.
- Santer, B. D., and Coauthors, 2005: Amplification of surface temperature trends and variability in the tropical atmosphere. *Science*, **309** (5740), 1551–1556.
- Vallis, G. K., P. Zurita-Gotor, C. Cairns, and J. Kidston, 2015: Response of the large-scale structure of the atmosphere to global warming. *Quart. J. Roy. Meteor. Soc.*, **141** (690), 1479–1501.